The Occurrence and Effect of Sulfate Reduction and Sulfide Oxidation on Coastal Limestone Dissolution in Yucatan Cenotes

by Ronald K. Stoessell[a], Yolanda H. Moore[b], and James G. Coke[c]

Abstract

Dissolution of carbonate minerals in the coastal halocline is taking place in the karst terrain along the northeastern coast of the Yucatan Peninsula. The dissolution is being accelerated in cenotes (sinkholes) where sulfate reduction and oxidation of the produced sulfide is occurring.

Hydrogen-sulfide concentrations ranged from 0.06 to 4 mmolal within the halocline in two sinkholes. Relative to concentrations expected by conservative mixing, fluids with high hydrogen-sulfide concentrations were correlated with low sulfate concentrations, high alkalinities, low pH values, and heavy sulfur isotope values for sulfate. Hydrogen-sulfide concentrations were less than those predicted from sulfate reduction, calculated from deficiencies in measured sulfate concentrations, indicating mobility and loss of aqueous sulfide.

Fluids with low hydrogen-sulfide concentrations were correlated with very high calcium concentrations, high strontium and sulfate concentrations, slightly elevated alkalinities, low pH values, and sea-water sulfur isotope values for sulfate. Gypsum dissolution is supported by the sulfur isotopes as the major process producing high sulfate concentrations. However, oxidation of aqueous sulfide to sulfuric acid, resulting in carbonate-mineral dissolution is needed to explain the calcium concentrations, low pH values, and only slightly elevated alkalinities.

The halocline may trap hydrogen sulfide that has been stripped from the underlying anoxic salt water. The halocline can act as a stable, physical boundary, holding some of the hydrogen sulfide until it is oxidized back to sulfuric acid through interaction with the overlying, oxygenated fresh water or through the activity of sulfide-oxidizing bacteria.

Introduction

The coastal halocline, the mixing zone of brackish water separating the fresh-water lens from the underlying sea water, is an environment in which limestone is commonly dissolved (e.g., Badiozamani, 1973; Plummer, 1975). This dissolution magnifies karst features in coastal limestones, e.g., the development of cenotes (sinkholes), fractures, and mega-porosity. This study reports the occurrence and effect of minor to moderate amounts of sulfate reduction and the oxidation of hydrogen sulfide to sulfuric acid on dissolution of coastal limestones positioned within the halocline.

Sulfate reduction produces aqueous sulfide, increases alkalinity, and lowers the pH. The pH will be increased by subsequent precipitation of iron sulfides or further lowered by back-oxidation of aqueous sulfide to sulfuric acid. These processes have been recently modeled in halocline fluids by Stoessell (1992). The overall results are dissolution of calcite and aragonite for minor to moderate sulfate reduction and when the aqueous sulfide is back-oxidized to sulfuric acid. Precipitation in halocline fluids occurs with major sulfate reduction and when iron sulfides precipitate. Recently, Smart et al. (1988) suggested that iron-sulfide precipitation and calcium-carbonate dissolution in the halocline in the Bahamas were due to sulfate reduction and sulfide oxidation.

Sinkholes along the northeastern coast of the Yucatan Peninsula (Figure 1) act as local basins for collecting organic debris which can be used in sulfate reduction. Two sinkholes, examined in this study, provide evidence for sulfate reduction, accumulation of hydrogen sulfide in the halocline, and oxidation of aqueous sulfide to sulfuric acid. The Pleistocene limestone aquifer, containing the sinkholes, is unconfined and highly fractured. The aquifer contains a thin halocline one to three meters thick (Figure 2).

The limestone is composed of low-Mg calcite and aragonite with minor amounts of Ca-rich dolomite which formed in the saline portion of the Pleistocene halocline (Ward and Halley, 1985). Iron sulfides have not been reported in the limestones. The aragonite is undergoing preferential dissolution in the mixing zone (halocline) of the

[a]Department of Geology and Geophysics, University of New Orleans, New Orleans, Louisiana 70148.
[b]1623 Lakeshore Drive, Mandeville, Louisiana 70448.
[c]Excursions Akunal, Postal 1, Playa del Carmen, Quintana Roo, Mexico 77710.

Received February 1992, revised July 1992 and January 1993, accepted February 1993.

fracture fluids (Back et al., 1986). The compositions of these "fast moving" fracture fluids and the observed aragonite dissolution in the saline portion of the mixing zone can be predicted by conservative mixing of coastal fresh-water and sea-water end members (Stoessell et al., 1989). The "slowly moving" pore fluids allow time for water-rock interaction. These fluids are close to equilibrium with aragonite in the low-salinity portion of the mixing zone, but are still undersaturated in the high-salinity portion of the mixing zone (Chen, 1991). The fluid-flow rates range from more than a cm per sec in the fracture fluids to at least two orders of magnitude lower in the pore fluids (Moore et al., 1992).

Chemistry of Sulfate Reduction and Related Reactions Affecting Alkalinity

Concentrations of aqueous sulfate, hydrogen sulfide, bicarbonate, nitrate, calcium, magnesium, and strontium are used in this study as evidence for sulfate reduction, oxidation reactions, and related fluid-rock reactions. These reactions are given below, and their effects on alkalinity are discussed later. Agreements between measured and predicted alkalinities are used to indicate how well we understand the geochemical system.

The **delta** concentration of an aqueous component (as used in this study) is the difference between the measured molality and the predicted molality due to conservative mixing of **pure water**, i.e., near rain-water composition, with **sea water**. The **delta** concentration is different from an **excess** or **deficient** concentration. An **excess** or **deficient** concentration refers to the difference between the measured molality and the predicted molality due to conservative mixing of **fresh water** with **sea water** to form the halocline. The fresh water entering the halocline is not rain water, because its composition has been modified by fluid-rock interactions and the absorption of carbon dioxide. The **delta** concentrations are used in this study to check for an alkalinity balance between predicted and measured alkalinities in fluids, whereas **excess** and **deficient** concentrations are used for evaluation of the effects of fluid-rock interactions and aqueous reactions.

The anaerobic aqueous sulfate reduction of terrestrial organic matter, e.g., leaves falling to the bottom of the cenotes, catalyzed by bacteria (*Desulfovibrio* sp.), can be written using the Deevy organic-matter composition $C_{882}H_{1794}O_{886}N_9SP$ (Morse and Mackenzie, 1990, p. 505). For simplicity, the elemental formula is divided by 441 and the overall reaction is split below into two separate reactions: an organic molecule represented by a carbohydrate CH_2O (Morse and Mackenzie, 1990, p. 505) and the residual nitrogen, phosphorus, hydrogen, and oxygen atoms (1/441) ($N_9H_{30}SPO_4$).

$$2CH_2O + SO_4^{2-} \Rightarrow 2HCO_3^- + H^+ + HS^- \quad (1a)$$

and

$$(1/441)\,[H_{30}N_9SPO_4 + H_2O] \Rightarrow (1/441)\,[9NH_3 + H_3PO_4 + 0.25SO_4^{2-} + 0.75HS^- + 1.25H^+]. \quad \ldots (1b)$$

In the presence of oxygenated waters, the hydrogen sulfide and ammonia may be oxidized to sulfuric and nitric acid, e.g.,

$$HS^- + 2O_2 \Rightarrow H^+ + SO_4^{2-} \quad (2a)$$

and

$$NH_3 + 2O_2 \Rightarrow H^+ + NO_3^- + H_2O \quad (2b)$$

No change in alkalinity occurs through the hydrolysis of hydrogen sulfide to form H_2S or through partial oxidation (with oxygen reduction) to produce sulfur. No change in alkalinity occurs through the partial oxidation of hydrogen sulfide to produce polysulfides, e.g., S_2^{2-}, assuming the polysulfide can accept H^+ ions to form H_2S and sulfur during an alkalinity titration. No changes in alkalinity occur through the dissolution of sulfate minerals.

The precipitation and dissolution of various carbonate minerals can be represented by the hydrolysis of the mineral components in solid-solution in calcite, aragonite, and dolomite:

$$CaCO_3 + H^+ \Leftrightarrow Ca^{2+} + HCO_3^-, \quad (3a)$$

$$MgCO_3 + H^+ \Leftrightarrow Mg^{2+} + HCO_3^-, \quad (3b)$$

and

$$SrCO_3 + H^+ \Leftrightarrow Sr^{2+} + HCO_3^-. \quad (3c)$$

The overall alkalinity difference from that predicted by conservative mixing of sea water with pure water of zero alkalinity, **delta alk** in meq/kg H_2O, is predicted by

$$\textbf{delta alk} = 2\,\textbf{delta(Ca + Mg + Sr)} - 2\,\textbf{delta SO}_4 \quad (4)$$

Equation (4) includes the effects of reactions (1a), (2a), and (3a), (3b), and (3c).

The **delta alk** in each of the field samples was predicted from equation (4) and compared with that computed from the measured alkalinity titrations of HCO_3^-, CO_3^{2-}, and HS^-. Precipitation of iron sulfides were not considered because they have not been reported in this study area (Ward and Halley, 1985; Ward, personal communication, 1992). Equation (4) does not consider the changes in alkalinity from the N and S in organic matter in reaction (1b) and the subsequent oxidation of NH_3 in reaction (2b). However, the N:S:C ratio in terrestrial organic matter of 9:1:882 is too low for the alkalinity to be significantly affected by organic nitrogen and sulfur. The low concentrations of nitrate and phosphate found in this study indicate a lack of other sources such as fertilizer.

Sample Methodology, Field, and Laboratory Procedures

The fluid samples were collected at several sites shown in Figure 1 at the end of the dry season in May 1991. Two of the sampling sites were on CALICA property which is 8 km south of Playa del Carmen. These were the P2 borehole and Little Cenote Calica which are 2.5 and 4.4 km, respectively, west of the coast. A third sampling site at Cenote Angelita was 12 km from the coast. A fourth sampling site was several km inland in the halocline of the Maya Blue submarine cave. A Caribbean Sea sample was taken at Playa del Carmen to serve as the sea-water end member.

Sampling depths were picked to bracket the halocline. The vertical extent of the halocline was determined from a

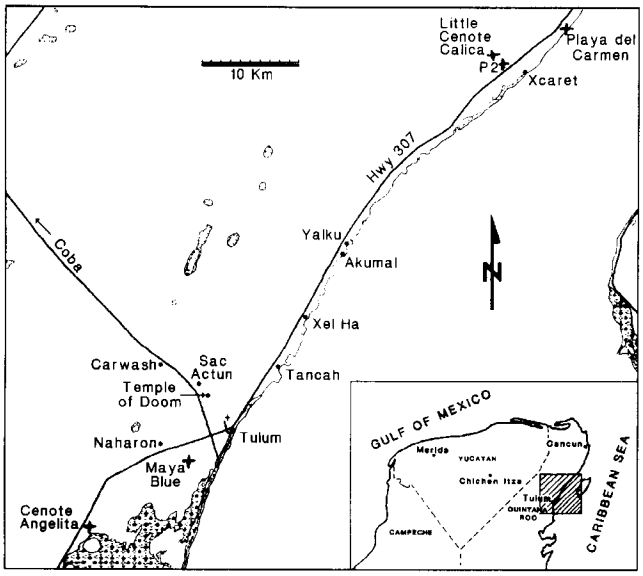

Fig. 1. Location map. Sample sites locations are marked with a + symbol.

conductivity profile run one day prior to sampling. A modified YSI model 3000 temperature-conductivity probe was used to make the three depth profiles shown in Figure 2. The "approximate" percent sea-water values in the profiles were computed assuming a linear relationship between conductivity and sea-water percentage. The depths on Figure 2 are relative to mean sea level. The changes in depth to the halocline between the sampling sites reflect differences in distance from the coast. Samples could not be taken below the halocline in Little Cenote Calica and Cenote Angelita due to obstructions and insufficient length of cable.

Each sample was collected in a 1 liter, stainless-steel sampler, which was lowered in an open position to the desired depth and closed by dropping a messenger. Stainless steel is chemically inert in the presence of aqueous sulfide for brief time periods at low temperatures (Martin Schooner, personal communication, 1992). The samples were collected progressively deeper to avoid disturbing the underlying water column. Sample collection took less than 5 minutes. The reported sample depths in Table 1 are relative to the water table.

The color of the unfiltered halocline samples from Cenote Angelita and Little Cenote Calica was reddish. During scuba diving in Cenote Angelita, white clouds, several feet in diameter, were observed floating in fresh water above the "red" halocline interface. The red color of the halocline and the white clouds in the fresh-water zone are thought to be due to either bacteria or algae. Subsequent SEM and EDS laboratory analyses of the filter paper used in filtering the red halocline samples did find trace amounts of diatoms and particulate mineral matter containing calcium and sulfur.

Water samples collected in April 1992 in the cenotes were tested for bacterial growth using selective agar for sulfide-oxidizing bacteria. Bacterial growth indicate the "probable" occurrence of *Thiobacillus* sp. bacteria throughout the water column, including the fresh-water zone (Walsh, Institute for Environmental Studies, LSU, personal communication, 1992). This conclusion is supported by the subsequent microbial production of particulate sulfur in the "acidified" filtered halocline water samples (rich in hydrogen sulfide), stored in the laboratory for several months. The sulfur was identified by SEM and EDS laboratory analyses.

The pH, temperature, and hydrogen sulfide (total aqueous sulfide) concentrations were measured on unfiltered samples a few minutes after collection. Eh was not measured but can be computed from the sulfide/sulfate redox couple, using the concentrations reported in Table 1 (Stumm and Morgan, 1981, pp. 490-494). The pH and temperature were measured using a Jenco Model 6009 pH Meter, calibrated between pH 4 and 7. The recorded temperatures correspond to the actual time of pH measurement and not the in situ values which were within 0.5° of 25.4°C. Hydrogen sulfide was measured using a sodium thiosulfate titration of an acidified sample treated with an excess of iodine solution (American Public Health Association, 1975, p. 504). Part of each sample was then filtered through a 0.45-μm filter and split into two aliquots for subsequent laboratory analyses, one of which was field-acidified with HCl to a pH of about two. The field alkalinity was measured on the nonacidified, filtered aliquot using a standard acid titration with HCl to a pH of 4.5 (American Public Health Association, 1975, p. 280).

Chemical laboratory procedures were those described by Stoessell et al. (1989) with the exceptions of phosphate and nitrate which were analyzed, respectively, by stannous-chloride reduction of molybdophosphoric acid, and by the nitrate-brucin reaction (American Public Health Association, 1975, pp. 427 and 479). Samples containing hydrogen sulfide were boiled to remove interferences before analyzing

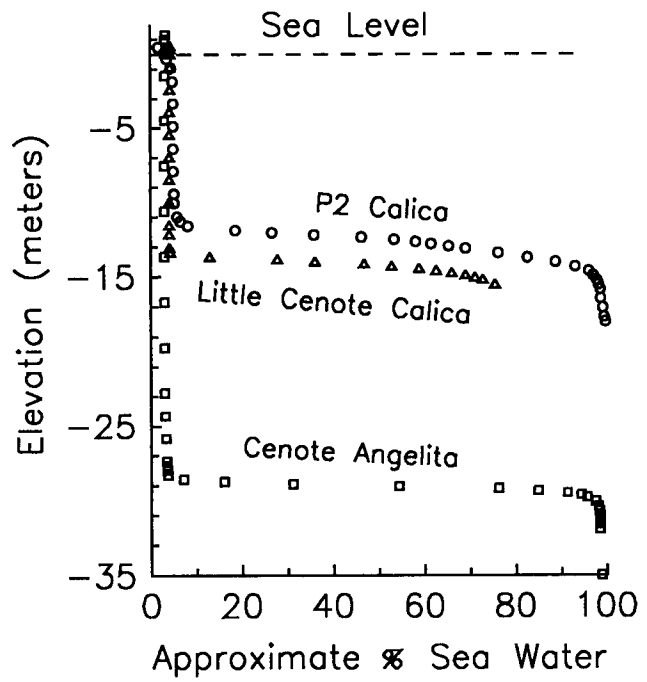

Fig. 2. Depth below mean sea level versus approximate percent sea water (from electrical conductivity measurements) at the sampling sites.

Table 1. Sample Data (May 1991)

Depth m[a]	Date & time	% s.w.	T° C[c]	pH	TDS ppm	Alk[f] meq/kg H_2O	SO_4	Cl	HS	NO_3	PO_4	SiO_2	Ca	Mg	K	Na	Sr	Fe[g]	Elec. bal. meq/kg H_2O	$\delta^{34}S$ in SO_4
							[					— mmolality						]		
Calica P2																				
3.8	7 AM 5/16	2.7	27.7	7.04	1,560	8.14	0.674	14.5	b.d.	0.11	0.0001	0.0635	3.07	2.06	0.282	12.6	0.0078	0.005	–0.9	n.m.
10.2	5 PM 5/15	3.0	28.3	6.92	1,600	6.73	0.782	16.1	b.d.	0.17	0.0003	0.0672	3.07	2.28	0.305	14.9	0.0066	0.005	+1.3	n.m.
13.0	6 PM 5/15	44.0	27.3	6.98	15,650	5.69	13.0	240.3	b.d.	0.079	0.0005	0.0440	6.74	24.1	4.52	206	0.0326	0.013	+0.2	n.m.
17.8	9 AM 5/16	97.8	28.0	7.35	33,790	2.53	28.2	543.7	b.d.	b.d.	0.0001	0.0153	10.5	51.9	10.1	467	0.0606	0.013	–0.6	18.6
Little Cenote Calica																				
6.0	4 PM 5/16	2.5	27.6	7.125	1,410	6.83	0.802	13.3	b.d.	0.15	0.0002	0.0580	2.97	1.95	0.226	11.0	0.0086	0.005	–0.8	n.m.
13.6	5 PM 5/16	2.0	27.2	7.15	1,300	6.66	0.760	10.6	b.d.	0.16	0.0002	0.0600	3.00	1.91	0.217	11.1	0.0086	0.005	+2.2	n.m.
14.4	4 PM 5/18	18.8	26.6	7.13	7,100	11.27	4.04	101.7	1.17	0.021	0.014	0.30[e]	4.93	11.4	1.64	84.6	0.0156	0.007	–2.1	n.m.
15.1	Noon 5/17	56.8	28.8	6.90	20,270	18.33	11.0	311.5	4.03	b.d.	0.025	0.61[e]	8.45	31.0	5.01	272	0.0308	0.009	+4.1	n.m.
15.9	3 PM 5/17	70.5	26.6	6.80	24,800	19.36	14.1	388.4	2.76	b.d.	0.020	0.65[e]	9.69	38.3	6.74	330	0.0351	0.009	–3.2	31.4
Cenote Angelita																				
22.9	4 PM 5/21	1.5	—[c]	6.95	1,110	7.15	0.435	8.22	b.d.	0.17	0.0012	0.113	3.17	1.30	0.118	6.97	0.0128	0.005	–0.3	n.m.
29.6[b]	9 AM 5/19	2.7	27.5	6.86	1,520	6.98	0.738	14.5	b.d.	0.11	0.0003	0.113	3.45	2.03	0.252	12.6	0.0139	0.004	+0.8	n.m.
30.2[b]	10 AM 5/19	33.2	27.8	6.77	12,180	6.65	11.0	180.7	0.061	b.d.	0.0003	0.141	8.84	17.1	3.00	155	0.0433	0.009	+0.6	18.7
30.5	3 PM 5/21	33.2	—[c]	6.86	12,000	6.65	10.4	180.7	0.061	b.d.	0.0003	0.138	8.66	17.8	3.13	149	0.0425	0.009	–3.0	18.6
31.1	5 PM 5/21	88.7	—[c]	6.86	31,650	4.54	31.7	491.9	0.275	b.d.	0.0015	0.18[e]	19.5	45.8	8.81	420	0.0991	0.009	–0.2	18.5
Maya Blue Cave																				
16.8[b]	Noon 5/18	90.1	28.5	7.15	31,180	2.94	26.1	499.4	b.d.	0.023	0.0003	0.0254	10.1	48.0	9.39	428	0.0568	0.006	–0.9	n.m.
Playa del Carmen Caribbean Sea Water																				
0.3[b]	6 PM 5/16	100.0	28.8	8.05	34,470	2.66	28.9	556.5	b.d.	b.d.	b.d.	0.0041	10.4	52.8	10.0	476	0.0580	0.006	–4.4	18.3

[a] Depth from center of 0.5 meter tube sampling interval below water table which was at 0.47 m and 0.58 m above mean sea level, respectively, at Calica P2 and Little Cenote Calica;
[b] Taken by diver at depth (using depth gauge) in bottle;
[c] Temperature at time of pH measurement; —[c] not recorded but between 27 and 28° C;
[e] Samples with detectable aqueous sulfide at the time of analyses in which the aqueous sulfide was removed by boiling;
[f] Includes Inorg. C and HS^- contributions but not $B(OH)_4^-$;
[g] Affected by sea-water matrix which increases apparent concentrations in the most saline samples;
b.d. Below detection (< 0.003, < 0.003, and < 0.0001 mmolality, respectively, for HS, NO_3, and PO_4);
n.m. Not measured.

for silicate and phosphate. The laboratory analyses, with the exceptions of phosphate and nitrate, were completed within a month of sampling. Nitrate and phosphate analyses were performed on filtered, acidified samples six months after collection. The field and laboratory chemical data are reported in Table 1. The estimated uncertainty of field pH is within 0.03 units, resulting from carbon dioxide degassing. Reproducibilities of the reported concentrations are within 3% for all components, except nitrate and sulfate which are within 5%.

The percent sea water of each sample was computed from the measured chloride concentrations, using conservative mixing of the Caribbean sea-water sample and a fresh-water end member having zero chloride concentration. The presence of trace chloride contents in fresh water, due to a trace chloride content in rain water, will not produce a significant error in the sea-water percent computation. Alkalinities have been reduced by estimated contributions from borate using the borate concentrations predicted from conservative mixing with standard sea water of $35^{0}/_{00}$ (ppt) salinity (Stumm and Morgan, 1981, p. 187).

$\delta^{34}S$ isotopes were run on sulfate in the halocline samples and the Caribbean sea water. The isotope analyses were conducted by Coastal Science Laboratories in Austin, Texas, with a reported accuracy within $0.5^{0}/_{00}$. The sulfur standard is the sulfur in the iron meteorite Canyon Diablo.

The filter papers used in filtering the red halocline samples from the cenotes were examined by an Amray Model 1820 scanning-electron microscope (SEM) with a Kevex energy-dispersive x-ray spectroscope (EDS).

Thermodynamics

The Fortran computer program REACT, described in Stoessell et al. (1989), was used to compute the saturation indices for various carbonate minerals. REACT uses the total solution composition (including alkalinity and pH) at a particular temperature and pressure to calculate total molalities of all thermodynamic components, including hydrogen and inorganic carbon. These data can then be used to calculate the activities of aqueous species at any temperature and pressure. The procedure involves calculation of an aqueous species distribution at the temperature and pressure of interest and includes the temperature and pressure dependence of the thermodynamic parameters and the calculation of activity coefficients. This procedure was used with field-sample data to correct to 25°C and 1 bar, and thereby allow comparison of samples taken at slightly different temperatures.

The definition of the saturation index **SI** is shown below, using calcite as an example. The **SI** for calcite is determined from the dissolution or hydrolysis reaction:

$$CaCO_3 + H^+ \Rightarrow Ca^{2+} + HCO_3^- \qquad (5)$$

as $$\mathbf{SI} = \log [(\mathbf{a}_{Ca^{2+}}\, \mathbf{a}_{HCO_3^-})/\mathbf{a}_{H^+}] - \log \mathbf{K}, \qquad (6)$$

where **K** is the reaction equilibrium constant and $\mathbf{a}_i$ is the activity of the ith aqueous species. A positive **SI** indicates supersaturation and a negative **SI** indicates undersaturation with respect to the mineral. The **SI** values for calcite and aragonite in diagrams within this paper are referenced to two different vertical axes representing mineral stability data from Plummer and Busenberg (1982) and from Robie et al. (1978). The difference between the two axes, marked **P** and **R**, respectively, represents the uncertainty in the stability of each mineral (Figure 4). For a discussion on general uncertainties due to errors in measured solution compositions and computation of aqueous activities, the reader is referred to Merino (1979).

The saturation indices for the Yucatan dolomite are relative to an estimated stability by Stoessell et al. (1989) for a disordered, Ca-rich, Pleistocene dolomite. The dolomite has a 25°C and 1 bar log K (equilibrium constant) of 3.99 for the following hydrolysis reaction:

$$Ca_{1.14}Mg_{0.86}(CO_3)_2 + 2H^+ = 1.14Ca^{2+} + 0.86Mg^{2+} + 2HCO_3^- \qquad (7)$$

Saturation indices for conservative mixing were derived in REACT in which the fresh-water end member was the most dilute sample taken from Cenote Angelita and the sea-water end member was the Caribbean sea-water sample. Each of the compositions on a mixing curve result from mixing different proportions of the two end members, using the concentrations of their aqueous components, including hydrogen ions, at 25°C and 1 bar.

Saturation indices were also computed in REACT for conservative-mixing compositions in which a "given" percentage of sulfate reduction had occurred in the sea-water end member. Some of these compositions also included oxidation of the produced hydrogen sulfide back to sulfuric acid. The sea-water composition was modified, using the stoichiometry of reaction (1a) for sulfate reduction and of reaction (2a) for hydrogen sulfide oxidation, assuming that the required organic matter and dissolved oxygen were available in the reactions.

The amounts of aragonite that could be dissolved or precipitated by the above solution compositions were also calculated in REACT. Aragonite was used, rather than the more stable polymorph calcite, because of the preferential dissolution of aragonite in the halocline (Back et al., 1986).

Results and Discussion

Data given in Table 1 are plotted versus percent sea water in Figure 3 for five of the chemical components and for pH. SI values for the samples and for conservative-mixing curves are plotted in Figure 4 for aragonite, "ordered-stoichiometric" dolomite, calcite, and "disordered Ca-rich" Yucatan dolomite. SI values for aragonite are plotted on Figure 5A for conservative-mixing curves, each characterized by a given amount of sulfate reduction. The dashed curves include back-oxidation of aqueous sulfide in the sea-water end member. The corresponding curves on Figure 5B indicate the amounts of aragonite dissolution (negative) or precipitation (positive) needed to equilibrate the solutions.

Three dashed-line trends are labeled on the diagrams in Figures 3 and 4, depending on the concentrations of hydrogen sulfide present (Figure 3C):

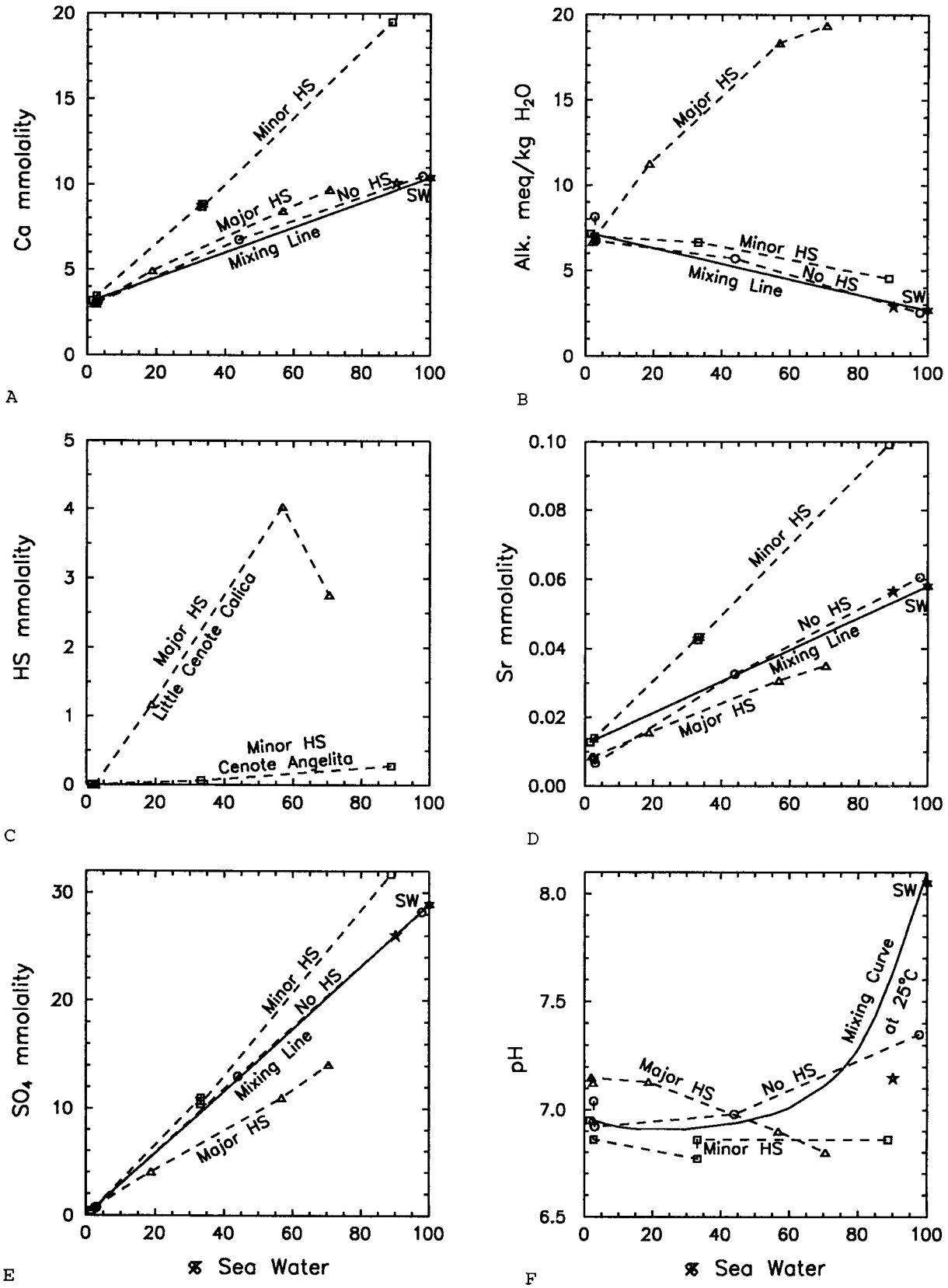

Fig. 3. Concentrations, alkalinities and pH values versus percent sea water at the sampling sites. The dashed lines and curves refer to sample trends, and the solid lines and curve represent conservative mixing with the Caribbean sea-water sample. The Maya Blue Cave sample symbol is a star. The No HS, Minor HS, and Major HS trends contain data, respectively, from the Calica P2 borehole, Little Cenote Calica, and Cenote Angelita.

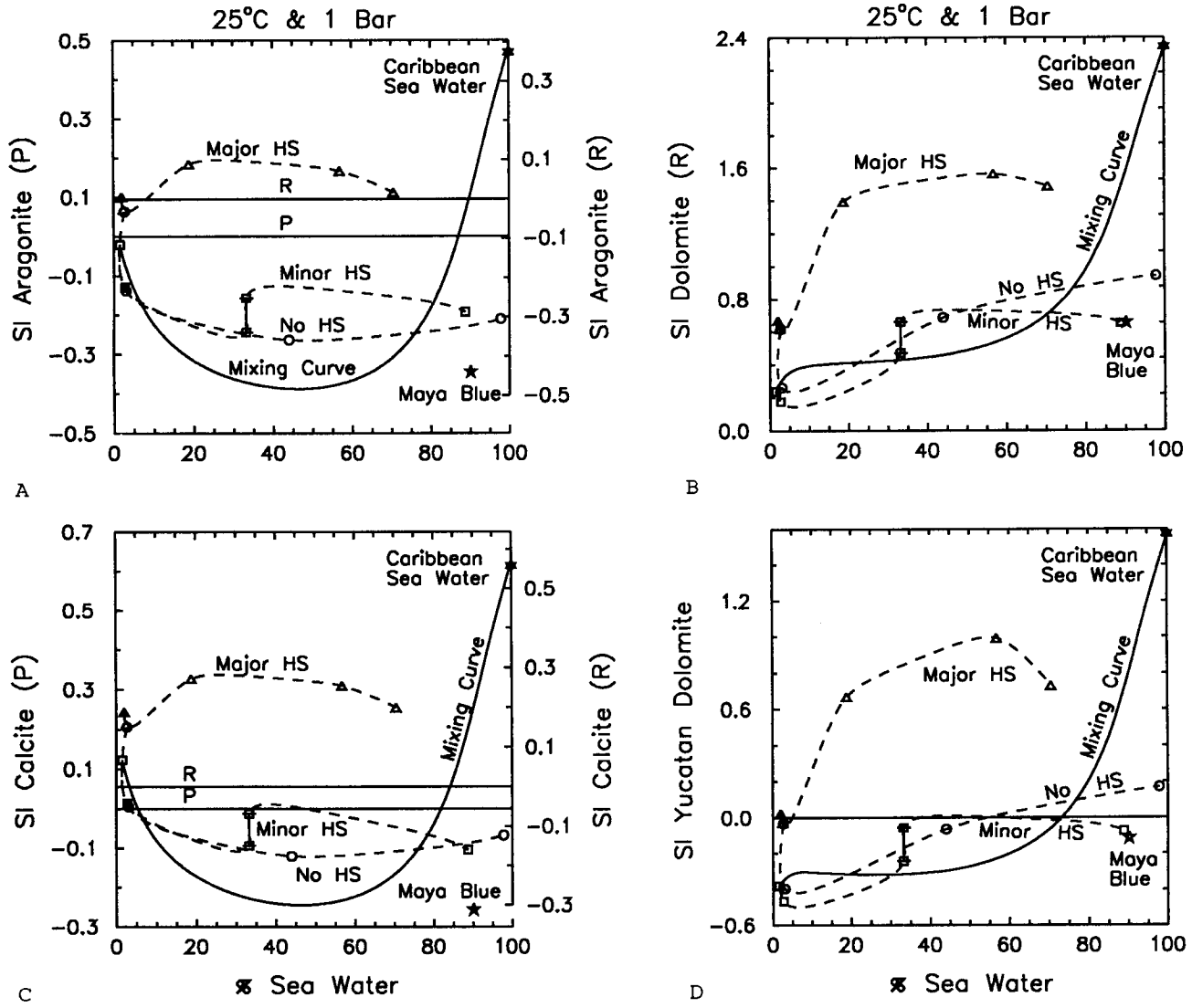

Fig. 4. Mineral SI values versus percent sea water at the sampling sites, relative to the aragonite stabilities of Plummer and Busenberg (1982) and Robie et al. (1978), marked "P" and "R," respectively. Sample data symbols plotted are as for Figure 3. Solid curves represent conservative mixing between the least saline sample from Cenote Angelita and the sea-water sample.

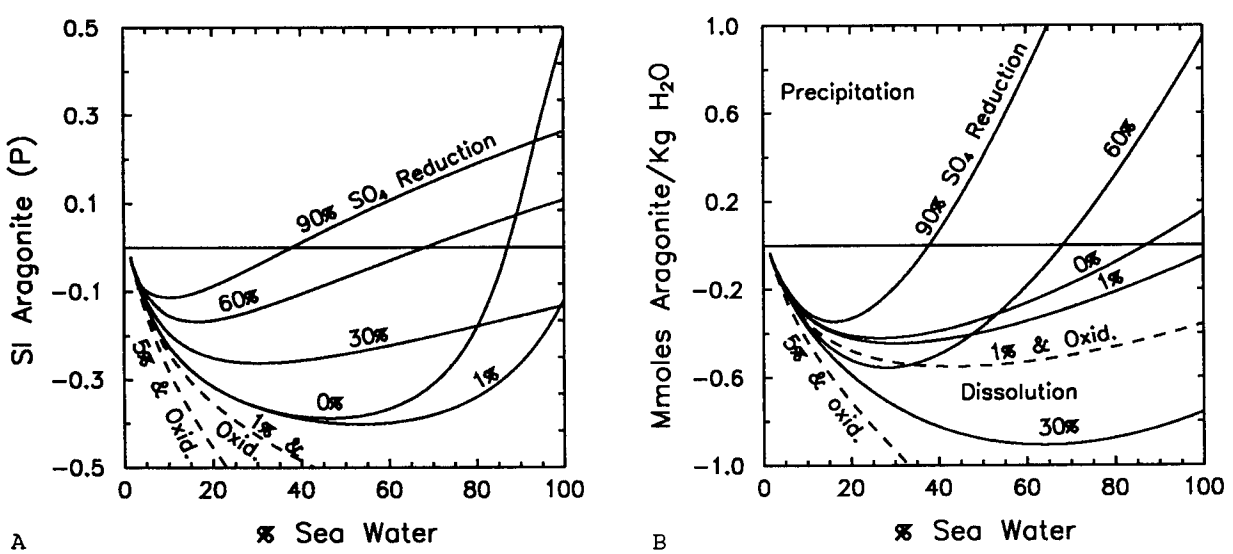

Fig. 5. Aragonite SI values are shown on Figure 5A for conservative-mixing curves in which the percent of sulfate reduction in the sea-water end member has been varied from 0 to 90%. The SI values on the two dashed curves result from oxidation of the produced hydrogen sulfide back to sulfate. The corresponding amounts of aragonite dissolution (negative amounts) or precipitation (positive amounts), needed to reach equilibrium, are shown on Figure 5B.

○ **No HS**: Calica P2 borehole samples;

□ **Minor HS**: Cenote Angelita samples having concentrations up to 0.3 mmolal; and

△ **Major HS**: Little Cenote Calica samples having concentrations up to 4 mmolal.

Hydrogen sulfide was not found in any samples in the fresh-water zone overlying the halocline (Table 1). As previously mentioned, samples could not be taken below the halocline, except in the Calica P2 borehole.

The data from samples for the submarine Maya Blue Cave (90% sea water) and from Playa del Carmen sea water are also plotted on Figures 3 and 4. The Maya Blue sample represents fracture fluids in the halocline in a noncenote environment. In Figure 3, these two samples plot on the "No HS" trend, except for the pH diagram on Figure 3F.

The conservative-mixing concentrations, pH values, and SI values, for mixing sea water with the most dilute fresh-water sample, are shown by the solid "mixing line" or "mixing curve" on the diagrams in Figures 3 and 4. On these diagrams in Figure 3, **excess** concentrations plot above the solid line, and **deficient** concentrations plot below the solid line.

No HS

The dashed line marking the **No HS** trend in the diagrams in Figure 3 appears to fall on or close to the mixing lines on Figure 3, apparently due to conservative mixing with less water-rock interaction than shown on the other trends. The $\delta^{34}S$ value in Table 1 for the aqueous sulfate is $18.6^{0}/_{00}$, implying nearly all of the sulfate is sea-water sulfate.

The lower-than-expected pH values in saline samples (Figure 3F) do not follow the conservative-mixing curve, resulting in these samples being undersaturated with respect to both aragonite (Figure 4A) and calcite (Figure 4C). Similar SI values were reported by Chen (1991) from Calica borehole samples taken in August 1990. These low pH values may be due to "minor" sulfate reduction of the order of 1% in the sea-water end member, combined with the subsequent removal of the hydrogen sulfide (since no HS was detected).

The effect of a 1% decrease in sulfate, due to sulfate reduction, is shown on "1%" conservative-mixing curve in Figure 5A. The SI values of the saline samples on the **No HS** trend on Figure 4A can be explained by this minor sulfate reduction. While a 1% decrease in sulfate concentrations is too small to be detected, the lower pH values will cause aragonite undersaturation, as shown in Figure 5A and discussed in Stoessell (1992).

Major HS

The **Major HS** trends in Figure 3 are associated with **excess** alkalinities (Figure 3B), **deficient** sulfate concentrations (Figure 3E), and **excess** phosphate concentrations (Table 1, halocline samples). The inverse relationship between **excess** alkalinities and **deficient** sulfate concentrations are predicted from sulfate reduction (reaction 1a). The heavy $\delta^{34}S$ value of $31.4^{0}/_{00}$ in the most saline sample (Table 1) is explained by $\delta^{34}S$ residual sulfate enrichment from the bacterial reduction of sulfate (Feely and Kulp, 1957). This enrichment is known to be variable, depending upon the rate of sulfate reduction (Faure, 1977, p. 404). The **excess** phosphate concentrations may also be related to sulfate reduction (reaction 1b).

The hydrogen-sulfide concentrations in the three samples from Cenote Calica are less than expected from the **deficiency** in sulfate concentrations [see reaction (1a) and Table 1]. The sulfate **deficiency** in the three samples changed from 26 to 33 to 31%, respectively, as sample depth increased from 14.4, to 15.1, to 15.9 m. The predicted **deficiency**, from the hydrogen sulfide concentrations, changed from 22 to 25 to 14%, over the same depth intervals. The hydrogen-sulfide concentrations are actually lower at the bottom of the halocline than in the middle of the halocline. Hydrogen sulfide is not conserved and is being removed more rapidly from the bottom than from the top of the halocline.

Calcium concentrations in Figure 3A in the **Major HS** trend are higher than those on the conservative-mixing line. Minor calcium-carbonate dissolution may have occurred. Dissolution of calcium-carbonate minerals is unexpected, since these samples are presently supersaturated (Figure 4). The supersaturation is at least partially due to moderate to major sulfate reduction in which alkalinity increases (Figure 3B) offset the lower pH values (Figure 3F). However, as shown in Figure 5A, for the moderate amount of sulfate reduction observed (about 30%), the halocline fluids should be able to dissolve aragonite, explaining the excess calcium concentrations. The reason for the present supersaturation is unknown; however, kinetic effects, perhaps related to the high phosphate concentrations, may have prevented calcium-carbonate mineral precipitation (Morse and Mackenzie, 1990, pp. 79 and 80).

Minor HS

The **Minor HS** trends in Figure 3 are characterized by **excess** calcium, strontium, and sulfate concentrations (Figures 3A, 3D, and 3E), minor **excess** alkalinities, and generally low pH values (Figure 3F). The concentrations and pH values are consistent with back-oxidation of hydrogen sulfide to sulfate and subsequent dissolution of calcite and aragonite. However, the $\delta^{34}S$ values of the halocline samples are those of sea water, indicating the sulfate increase is due primarily to gypsum dissolution. Gypsum dissolution is supported by SEM identification of the presence of fine-grained particles, containing calcium and sulfur, on filter papers used in filtering the halocline samples.

How can the **excess** calcium be explained? These excesses are approximated by the differences between the **Minor HS** trend and the mixing line on Figures 3A and 3E. Based on the **excess** in sulfate concentrations, about half of the **excess** in calcium could be due to gypsum dissolution. The remaining **excess** calcium and all of the strontium would be the result of calcite and aragonite dissolution (computed from data in Table 1).

The low pH, low alkalinities, and minor amounts of hydrogen sulfide must reflect minor sulfate reduction, followed by hydrogen sulfide oxidation to sulfuric acid to promote the dissolution of calcium-carbonate minerals. The

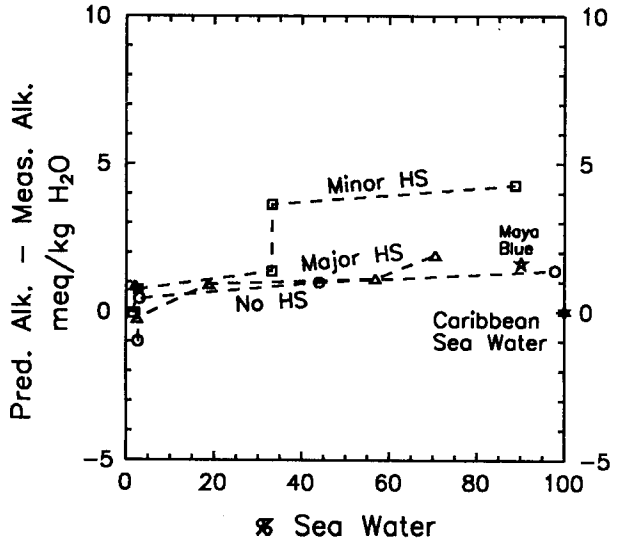

Fig. 6. Alkalinity balance between predicted alkalinities and measured alkalinities, computed using equation (4).

5% sulfate reduction with hydrogen sulfide oxidation curve on Figure 5B indicates aragonite can be dissolved on the order of mmoles per kg H_2O through the oxidation of minor amounts of hydrogen sulfide. The modeling curves on Figure 5B support hydrogen sulfide oxidation as a valid mechanism capable of dissolving sufficient aragonite to provide the measured calcium concentrations.

Although gypsum has been reported elsewhere in lower Eocene rocks in the Yucatan Peninsula (Lesser and Weidie, 1988), gypsum and anhydrite have not been reported in the younger limestones of northeastern Yucatan Peninsula (Lauderdale et al., 1979; Ward and Halley, 1985). The source of the particulates (reported above) containing calcium and sulfur in the halocline is not known, and the halocline samples were undersaturated with respect to gypsum.

The source of **excess** sulfate is not within the fresh-water zone. Samples taken at depths of 22.9 and 29.6 m in fresh water at Cenote Angelita show no **excess** sulfate (Figure 3E), whereas samples taken immediately below the fresh-water zone in the halocline at 30.2, 30.5, and 31.1 m have **excess** sulfate. The increase in calcium concentration (with increasing salinity) is almost linear across the halocline (Figure 3A), implying conservative mixing between the sea-water and fresh-water end members without significant dissolution of gypsum and calcium carbonate. The **excess** calcium and most of the **excess** sulfate were derived by mineral dissolution in the sea-water zone. This sea water is part of a convection cell, in which saline water moves upward because of changes in density through the formation of the halocline (Moore et al., 1992).

The change in alkalinity is not as linear as the change in calcium across the halocline, implying that a nonconservative process is modifying the alkalinity. Consistent with the modeling discussed above, we believe this process includes minor oxidation of hydrogen sulfide to sulfate. Because the **excess** calcium originated below the halocline, most of the oxidation to sulfate occurred within the anoxic sea-water zone, possibly through the activity of sulfide-oxidizing bacteria. Bacterial growth on selective agar suggests the presence of *Thiobacillus* sp. and other sulfide-oxidizing bacteria throughout the water column.

We hypothesize that hydrogen sulfide may be stripped from the underlying anoxic waters, possibly through the formation of bubbles. The hydrogen sulfide is then collecting in the halocline where it is eventually oxidized to sulfuric acid, either by interaction with the overlying, oxygenated waters or by the activity of sulfide-oxidizing bacteria. The density gradient in the halocline acts as the barrier to the upward migration of hydrogen sulfide.

Alkalinity Balance

An alkalinity balance is shown in Figure 6. The sample **delta** alkalinity computed from the measured alkalinity is subtracted from the **delta** alkalinity predicted in equation (4), using the data in Table 2. Good agreement is shown for the **No HS** and **Major HS** trends; however, the predicted alkalinities are several meq/kg H_2O higher than the measured alkalinities for the **Minor HS** trend.

The alkalinity difference is not due to assuming gypsum dissolution because this process adds both calcium and sulfate, and does not change the **delta** alkalinity predicted from equation (4). Furthermore, partial oxidation of hydrogen sulfide to sulfur and/or polysulfides, and hydrolysis of hydrogen sulfide to H_2S gas should not change the alkalinity. The reason is unclear why the predicted alkalinities are several meq/kg H_2O higher than the measured alkalinities in the **Minor HS** trend.

Summary

Significant hydrogen-sulfide concentrations were found within the halocline in two coastal Yucatan sinkholes. The concentrations are evidence for the occurrence of sulfate

Table 2. Predicted Excess Alkalinity Minus Measured Excess Alkalinity

Bal = 2 Delta (Ca + Mg + Sr) − 2 Delta SO_4 − Delta Alk

m below w.t.	*% s.w.*	*meq/ kg H_2O*		*mmolality*				*meq/ kg H_2O*
Calica P2								
3.8	2.7	**-1.00**	=	6.86	+	0.21	−	8.07
10.2	3.0	**+0.44**	=	6.92	+	0.17	−	6.65
13.0	44.0	**+0.99**	=	6.08	−	0.57	−	4.52
17.8	97.8	**+1.39**	=	1.19	+	0.13	+	0.07
Little Cenote Calica								
6.0	2.5	**-0.23**	=	6.69	−	0.16	−	6.76
13.6	2.0	**+0.88**	=	7.31	−	0.36	−	6.07
14.4	18.8	**+0.93**	=	8.91	+	2.79	−	10.77
15.1	56.8	**+1.12**	=	7.11	+	10.83	−	16.82
15.9	70.5	**+1.92**	=	6.86	+	12.54	−	17.48
Cenote Angelita								
22.9	1.5	**-0.04**	=	7.07	−	0.00	−	7.11
29.6	2.7	**+0.75**	=	7.58	+	0.08	−	6.91
30.2	33.2	**+1.38**	=	9.96	−	2.81	−	5.77
30.5	33.2	**+3.62**	=	11.00	−	1.61	−	5.77
31.1	88.7	**+4.27**	=	18.58	−	12.13	−	2.18
Maya Blue Cave								
16.8	90.1	**+1.66**	=	2.32	−	0.12	−	0.54

reduction and related reactions which cause limestone dissolution in the sinkholes. The organic debris that collects in the sinkholes makes them an ideal environment for sulfate reduction.

Several trends were delineated, based on the maximum concentrations of hydrogen sulfide: a **No HS** trend in a borehole, and **Minor HS** and **Major HS** trends in the two sinkholes. The **No HS** trend appears to approximate conservative mixing with the exception of the low pH values. These pH values can be explained by minor 1% sulfate reduction followed by the loss of the hydrogen sulfide.

The **Major HS** trend shows evidence for major sulfate reduction and minor limestone dissolution. The halocline fluids have high hydrogen-sulfide concentrations and alkalinities, low sulfate concentrations with enriched $\delta^{34}S$ values, and calcium concentrations higher than expected by conservative mixing.

The **Minor HS** trend shows evidence for both gypsum and limestone dissolution with some oxidation of hydrogen sulfide to sulfate. The trend has higher sulfate, calcium, and strontium concentrations than expected from conservative mixing of sea water and fresh water, and has low pH values and low concentrations of hydrogen sulfide. The $\delta^{34}S$ values in the halocline support gypsum dissolution as the major reason for the high sulfate concentrations. Dissolution of calcium-carbonate minerals is needed to explain much of the higher calcium concentrations. Oxidation of hydrogen sulfide to sulfuric acid is needed to provide the low pH chemical environment for limestone dissolution without producing high alkalinities.

An unexplained deficiency in measured alkalinities occurs in the **Minor HS** trend, relative to alkalinities predicted by sulfate reduction, together with oxidation and various fluid-mineral reactions. Reasonable agreement exists between measured and predicted alkalinities in the **No HS** and **Major HS** trends.

Results from this study suggest that some hydrogen sulfide, generated by sulfate reduction in the anoxic waters below the halocline, has moved up into the halocline. There, interactions with the overlying, oxygenated water and/or the activity of sulfide-oxidizing bacteria have oxidized some of the aqueous sulfide to sulfate.

Acknowledgments

John Clark provided access to CALICA sites, and Jorge Rodriguez Bremauntz helped collect the CALICA data. Maud Walsh grew bacteria on selected agar for water samples collected from the cenotes in 1992. Partial field support was provided by Exxon Production Research Company and by Amoco Production Company. National Science Foundation Grants EAR-85 19368 and EAR-86 13639 provided funds to purchase the atomic-absorption spectroscopy system and the scanning-electron spectroscopy system used in this study at the University of New Orleans. Three anonymous reviewers of *Ground Water* provided detailed and useful suggestions and corrections on revising the manuscript.

References

American Public Health Association. 1975. Standard Methods for the Examination of Water and Wastewater (14th Edition). Washington, DC. 1193 pp.

Back, W., B. B. Hanshaw, J. S. Herman, and J. N. Van Driel. 1986. Differential dissolution of a Pleistocene reef in the ground-water mixing zone of coastal Yucatan, Mexico. Geology. v. 14, pp. 137-140.

Badiozamani, K. 1973. The *dorag* dolomitization model—Application to the Middle Ordovician of Wisconsin. Journal of Sedimentary Petrology. v. 43, pp. 965-984.

Chen, Y. 1991. Water chemistry of pore fluids in the coastal mixing zone, northeastern Yucatan Peninsula, Mexico. M.S. thesis. Univ. of New Orleans. 50 pp.

Faure, G. 1977. Principles of Isotope Geology. John Wiley, New York, NY. 464 pp.

Feely, H. W. and J. L. Kulp. 1957. The origin of the Gulf Coast salt dome sulfur deposits. American Assoc. of Petroleum Geologists Bulletin. v. 41, pp. 1802-1853.

Lauderdale, R. W., W. C. Ward, and A. E. Weidie. 1979. Carrillo Puerto Formation of northeastern Quintana Roo, Mexico. Gulf Coast Assoc. of Geological Societies Transactions. v. 29, pp. 275-280.

Lesser, J. M. and A. E. Weidie. 1988. Region 25, Yucatan Peninsula. In: Back, W., J. S. Rosenshein, and P. R. Seaber, eds., Hydrogeology. Geological Society of America, Boulder, CO, The Geology of North America. v. O-2, pp. 237-241.

Merino, E. 1979. Internal consistency of a water analysis and uncertainty of the calculated distribution of aqueous species at 25° C. Geochimica et Cosmochimica Acta. v. 43, pp. 1533-1542.

Moore, Y. H., R. K. Stoessell, and D. H. Easley. 1992. Freshwater/sea-water relationship within a ground-water flow system, northeastern coast of the Yucatan Peninsula. Ground Water. v. 30, pp. 343-350.

Morse, J. W. and F. T. Mackenzie. 1990. Geochemistry of Sedimentary Carbonates. Elsevier, New York, NY. 707 pp.

Plummer, L. N. 1975. Mixing of sea water with calcium carbonate ground water. In: Whitten, E.H.T., ed., Quantitative Studies in Geological Sciences. Boulder, CO, Geological Society of America Memoir 142. pp. 219-236.

Plummer, L. N. and E. Busenberg. 1982. The solubilities of calcite, aragonite, and vaterite in CO_2-H_2O solutions between 0 and 90° C, and an evaluation of the aqueous model of the system $CaCO_3$-CO_2-H_2O. Geochimica et Cosmochimica Acta. v. 46, pp. 1011-1040.

Robie, R. A., B. S. Hemingway, and J. R. Fisher. 1978. Thermodynamic properties of minerals and related substances at 298.15° K and 1 bar pressure and at higher temperatures. U.S. Geological Survey Bulletin 1452. 456 pp.

Smart, P. L., J. M. Dawans, and F. Whitaker. 1988. Carbonate dissolution in a modern mixing zone. Nature. v. 335, pp. 811-813.

Stoessell, R. K. 1992. Effects of sulfate reduction on $CaCO_3$ dissolution and precipitation in mixing-zone fluids. Journal of Sedimentary Petrology. v. 62, pp. 873-880.

Stoessell, R. K., W. C. Ward, B. H. Ford, and J. C. Schuffert. 1989. Water chemistry and $CaCO_3$ dissolution in the saline part of an open-flow mixing zone, coastal Yucatan Peninsula, Mexico. Geological Society of America Bulletin. v. 101, pp. 159-169.

Stumm, W. and J. J. Morgan. 1981. Aquatic Chemistry: An Introduction Emphasizing Chemical Equilibria in Natural Waters. Wiley-Interscience, New York, NY. 780 pp.

Ward, W. C. and R. B. Halley. 1985. Dolomitization in a mixing zone of near seawater composition, late Pleistocene, northeastern Yucatan Peninsula. Journal of Sedimentary Petrology. v. 55, pp. 407-420.